CHAPTER 82

NEAR-BOTTOM VELOCITIES IN WAVES WITH A CURRENT

by W.T. Bakker[1] and Th. van Doorn[2]

0 Abstract

Bakker (1974) developed a mathematical model concerning the sand concentration and velocity distribution in an oscillatory turbulent flow, with or without resultant current.

The flow is assumed to be uniform in horizontal direction. The present paper reports on an experimental verification of this theory. Furthermore, the numerical accuracy of the model has been investigated and diagrams are presented which enable the computation by hand of global velocity profiles.

1 Introduction

This paper deals with a numerical theory on the near-bottom velocity pattern in parallel-directed waves and current and with the comparison of theory and measurements. The paper is a sequence to an earlier paper (Bakker, 1974); the numerical theory concerning the velocity field developed herein is further refined and, in some respects, revised. For the sake of physical understanding an additional paper, dealing with an approximate analytical theory is in preparation (Bakker, 1979).

Furthermore, a Report is in preparation (Bakker and Van Doorn, 1979) which comprises as well the analytical and the numerical theory, and which goes further into details. This study has to be placed in a general scope of investigations, mentioned in the preceding paper (Bakker, 1974).

The necessary assumptions are mentioned in Ch. 2; in Ch. 3 the mathematical formulation is given. Because several aspects differ from those in the earlier paper, most of the derivations from this paper are repeated for convenience. Ch. 4 deals with the investigations on numerical accuracy. In Ch. 5 experiments are described, carried out in the Delft Hydraulics Laboratory (DHL). Comparison between theory and experimental data is made in Ch. 6. The present theory and the theory of Lundgren (1972) are compared in Ch. 7. After the conclusions (Ch. 8) the acknowledgements (Ch. 9), the literature and the symbols are mentioned.

The theory was developed by the first author; the experimental verification was carried out by the second author, who also reported on this subject.

2 Assumptions

The following assumptions are made:

a. Apart from turbulent fluctuations a horizontally directed and horizontally uniform current pattern is assumed. The current u is assumed to be only a function of the vertical coordinate z and the time t, but no function of the horizontal coordinate x.

---

[1] Senior Scientific Officer, Technical University of Delft

[2] Head of Study Dept. Vlissingen, Rijkswaterstaat, Netherlands
Project Engineer, Delft Hydraulics Laboratory, Netherlands

b. In the fluid a turbulent shear stress is assumed, according to the assumptions of Prandtl (1931) equal to:

$$\tau = \rho \ell^2 \frac{\partial u}{\partial z} \left| \frac{\partial u}{\partial z} \right| \tag{1}$$

in which τ is the shear stress, positive when acting in positive direction from the upper layer on the lower layer, ρ is the specific density of the fluid and ℓ is the mixing length.

c. A reasonable assumption on this mixing length and the distribution of the shear stress as a function of the height is obtained as follows. The equation of motion reads:

$$\rho \frac{\partial u}{\partial t} = \frac{\partial \tau}{\partial z} - \frac{\partial p_r}{\partial x} \tag{2}$$

in which p_r denotes the fluid pressure. A periodical water motion with period T is assumed. By Fourier analysis, one finds that the left-hand side of Eq. (2) will be zero when averaged over period T.
Then one finds from (2):

$$\frac{d\bar{\tau}_{real}}{dz} = \frac{\partial \bar{p}_r}{\partial x} \tag{3}$$

The bar above the symbol indicates the averaging over the wave period T; the subscript "real" of τ serves as a distinction from the schematized τ, mentioned later on.
Assuming, that the mean pressure gradient is constant over the height h, one may write for $\bar{\tau}$:

$$\bar{\tau}_{real} = (h-z) \frac{\partial \bar{p}_r}{\partial x} \tag{4}$$

If only a stationary and no periodic motion would occur, according to well-known methods one finds a logarithmic velocity distribution, starting from a mixing length ℓ_{real} according to:

$$\ell_{real} = \kappa z \sqrt{1 - \frac{z}{h}} \tag{5}$$

where κ is the Von Karman constant.
For a stationary current, this logarithmic velocity distribution is found also, if the shear stress $\bar{\tau}$ is schematized as a constant (i.e. uniform over the height):

$$\bar{\tau} = h \frac{\partial \bar{p}_r}{\partial x} \tag{6}$$

and the mixing length according to:

$$\ell = \kappa z \tag{7}$$

As the investigated features occur quite near to the bottom, where (4) and (6) on one hand and (5) and (7) on the other hand look very much the same, in the following the relationships (6) and (7) will be assumed.

d. Starting from a mixing length according to (7), generally it will be assumed, that the pressure gradient grad (p_r) is horizontally directed, i.e. that the pressure is only a function of x and t.

e. The mean velocity, when averaged over the water depth and the wave period is called U_{mean}. It is further assumed that the water mass far from the bottom is in oscillatory motion according to:

$$U_{osc} = \hat{U}_1 \sin(\omega t - \Psi_1) + \hat{U}_2 \sin(2\omega t - \Psi_2) + \hat{U}_3 \sin(3\omega t - \Psi_3) + \ldots \quad (8)$$

$\hat{U}_{mean}$, $\hat{U}_1$, $\hat{U}_2$, $\hat{U}_3$, Ψ_1, Ψ_2 and Ψ_3 can be arbitrary chosen. Connected with the solution, a small parasitary fourth harmonic is found, being 5 to 10% of the first one.
A solution with U_{mean} equal to zero can only be found, when also $\hat{U}_2$ is zero (as all higher even harmonics). In this case, a parasitary fifth harmonic of the order of 5 to 10% of the first one is found.

f. A hydraulically rough bottom is assumed. The velocity at a height z_o above the theoretical bottom level is assumed to be zero; it is assumed that z_o equals 1/33 times the Nikuradse roughness r.

3 Computation of water velocities and shear stress

Define a rather arbitrary height z_{max} above the bottom, in this way, that the periodical changes of the shear stress are attenuated at that height. For $z \geq z_{max}$ the shear stress τ equals $\bar{\tau}$, being assumed constant over the height (assumption c). Thus one finds from (2):

$$\rho \frac{\partial u}{\partial t} = - \frac{\partial p_r}{\partial x} \quad \text{for } z \geq z_{max} \quad (9)$$

Let the velocity at $z = z_{max}$ be U. Thus Eq. (9) remains valid, when u is replaced by U; let Eq. (9a) be Eq. (9) for u = U.
Define a "defect velocity" u_d as:

$$u_d = u - U \quad (10)$$

According to assumption d, subtracting Eq. (9a) from Eq. (9) yields:

$$\frac{\partial u_d}{\partial t} = 0 \quad \text{for } z \geq z_{max} \quad (11)$$

In (1), one may replace u by u_d, because U is no function of z. Thus, from (1) and (7) can be derived:

$$\bar{u}_d = \frac{\sqrt{\bar{\tau}/\rho}}{\kappa} \ln \frac{z}{z_{max}} \quad \text{for } z \geq z_{max} \quad (12)$$

Consider now the area where $z < z_{max}$. Subtracting Eq. (9a) from Eq. (2) and substituting u_d from (10) yields:

$$\frac{\partial u_d}{\partial t} = \frac{\partial(\tau/\rho)}{\partial z} \quad (13)$$

This equation can be transferred in an equation with the shear stress velocity p as independent variable.
Define p as:

$$p = \text{sign}(\tau) \cdot \sqrt{|\tau/\rho|} \quad (14)$$

Inversely, this implies:

$$\tau = \rho\, p|p| \quad (15)$$

From (1) and (7) it shows:

$$p = \kappa z \frac{\partial u}{\partial z} \tag{16}$$

In (16) one may replace u by u_d. Differentiation of (13) to z and multiplying with κz yields:

$$\frac{\partial p}{\partial t} = \kappa z \frac{\partial^2 (p|p|)}{\partial z^2} \tag{17}$$

For method of computation of u from p is referred to Bakker (1974). The following mainly deals with deviations from this paper. From p, one can find u_d with the aid of (10), which can be written as:

$$u_d = -\frac{1}{\kappa} \int_z^{z_{max}} \frac{p}{z} \, dz \tag{18}$$

Eq. (17) can be made dimensionless by introducing the following dimensionless variables:

$$\left.\begin{aligned} p^* &= p/\hat{p}_{b1} \\ t^* &= t/T \\ z^* &= z/Z, \text{ with } Z = \kappa \hat{p}_{b1} T \\ u^* &= u/\hat{p}_{b1} \quad \text{(see note 1))} \end{aligned}\right\} \tag{19}$$

in which $\hat{p}_{b1}$ is the amplitude of the first harmonic of the shear stress velocity at the bottom (the index "b" refers to "bottom").

Thus one obtains from (17):

$$\frac{\partial p^*}{\partial t^*} = z^* \frac{\partial^2 (p^*|p^*|)}{\partial z^{*2}} \tag{20}$$

As lower boundary condition is assumed:

$$p_b^* = \bar{p}_b^* + \sin 2\pi t^* + \hat{p}_{b2}^* \sin(4\pi t^* - \phi_2) + \hat{p}_{b3}^* \sin(6\pi t^* - \phi_3) \quad \text{for } z^* = 0 \tag{21}$$

If U_{mean} equals zero, $\bar{p}_b^*$ and $\hat{p}_{b2}^*$ are assumed zero; to the choice of the variables $\bar{p}_b^*$, $\hat{p}_{b2}^*$, $\hat{p}_{b3}^*$, ϕ_2 and ϕ_3 will be referred.

The upper boundary condition is determined by the fact that $\bar{\tau}$ should remain constant over the height according to (6)[2]; Averaging Eqs. (13) and (17) over the wave period (in which case the left-hand side becomes zero, as can be seen by decomposing u_d and p in harmonics) one finds that

---

[1] Generally, the velocities denoted by a symbol with an added star have been divided by $\hat{p}_{b1}$.

[2] J. van Overeem drew the attention of the author to the fact, that this condition was not fulfilled by the solution for waves and currents, given by Bakker (1974). Therefore the solution in the present paper contains a revision of last-mentioned paper with respect to the case of waves with a current.

the solution of these equations fulfills this condition automatically, if the upper boundary condition is properly chosen. At the upper boundary the shear stress velocity p should be equal to $\sqrt{\bar{\tau}/\rho}$:

$$p^* = \sqrt{\bar{p}_b^* \, |p_b^*|} \quad \text{for } z^* = z^*_{max} \tag{22}$$

In the case of an oscillatory flow without current (22) degenerates to $p^* = 0$ for $z^* = z^*_{max}$. In the computer program, initially an approximation is chosen according to:

$$p^* = \sqrt{\pi \bar{p}_b^* / 4} \quad \text{for } z^* = z^*_{max} \text{ (initially)} \tag{23}$$

This approximation follows from analytical considerations (Bakker, 1979). In the course of the computations, the real value of the right-hand side of (22) is calculated; after each period the upper boundary condition is adapted. This condition changes, because after some periods $\bar{p}_b^*$, $\hat{p}_{b2}^*$, $\hat{p}_{b3}^*$, ϕ_2 and ϕ_3 are adapted by means of an iterative procedure[1], in this way that the upper boundary condition (8) (in dimensionless shape) is fulfilled as good as possible.
In order to check the accuracy of this upper boundary condition, from the shear stress velocity p^* the value of U^* is calculated after some periods by means of numerical integration[1] with the aid of (18), which clearly keeps its validity in the dimensionless shape.

In the following, some attention will be paid to the results with respect to the first harmonic and the mean velocity profile. This gives just a general scope: solutions, which fit rather closely to the wanted boundary conditions can be found by application of the computer program.

With respect to the first harmonic, the dimensionless relationship between $\hat{u}_{d1}^*$ (the amplitude of the first harmonic of the dimensionless defect velocity) and z^* can be transferred into a dimensionless relationship between a kind of friction coefficient $\hat{p}_{b1}/\hat{U}_1$ and a_1/r, in which a_1 equals $\hat{U}_1 T/2\pi$ and r the Nikuradse roughness. This can be performed as follows.

Consider a certain defect velocity field u_d^*, which has been calculated, starting from certain bottom boundary conditions, defined by harmonics of p_b^*.

In principle every level z^* (at which u_d^* has been calculated) can be taken as a bottom boundary level z_o^*, where u^* is assumed zero. Therefore according to (10) the choice of z_o^* determines U^*, the dimensionless velocity far from the bottom (at $z^* = z^*_{max}$). Thus one computation of u_d^* determines a great number of velocity fields u^* with various upper boundary conditions and various values of z_o^*. Neglecting (just for the general scope) non-linear interactions between the harmonics of p^*, in first approximation the relationship between dimensionless first harmonic U_1^* and z_o^* can be investigated by taking $\bar{p}_b^*$, $\hat{p}_{b2}^*$ and $\hat{p}_{b3}^*$ in

---

[1] cf. Bakker (1974) and Bakker and Van Doorn (1979)

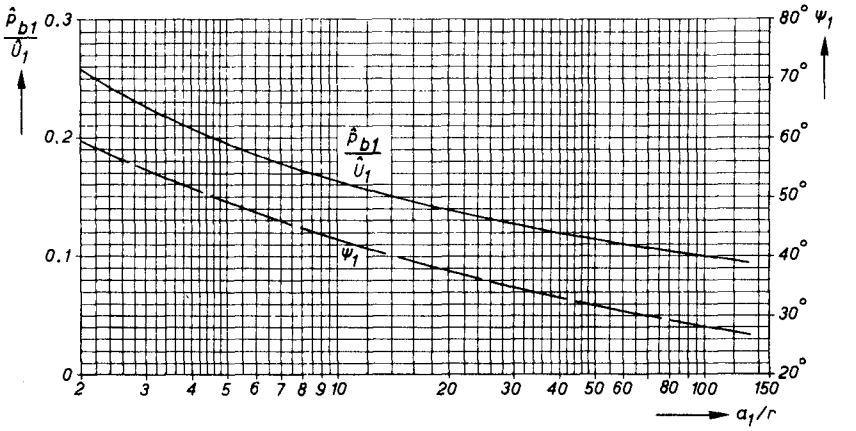

Fig.1. Ratio $\hat{p}_{b1}/\hat{U}_1$ between the amplitudes of the first harmonics of the shear stress velocity and the velocity far from the bottom, respectively phase lag Ψ_1 between $\hat{p}_{b1}$ and $\hat{U}_1$ as function of the ratio a_1/r between the stroke length and the ripple height.

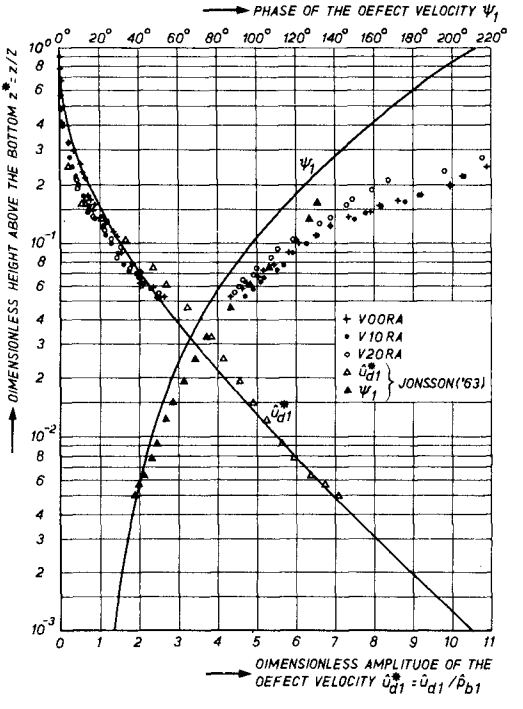

Fig.2. Dimensionless amplitude $\hat{u}^*_{d1}$ and phase Ψ_1 of the defect velocity as function of the dimensionless height above the bottom: according to theory and measurements.

(21) equal to zero and calculating u_d^* under these conditions.[1] On the effect of non-linear interaction will be returned in Ch. 4.

From assumption f and (19) the following relationship can be determined:

$$\frac{a_1}{r} = \frac{1}{66\pi K} \cdot \hat{U}_1^* / z_o^* \tag{24}$$

which in turn can be written, using (10):

$$\frac{a_1}{r} = \frac{1}{66\pi K} \hat{u}_{d1}^*(z_o^*)/z_o^* \tag{25}$$

where $\hat{u}_{d1}^*(z_o^*)$ denotes $\hat{u}_{d1}^*$ at the height z_o^*.

Now the ratio $\hat{p}_{b1}/\hat{U}_1$, relating the amplitude of the first harmonic of the bottom shear stress velocity to the amplitude of the first harmonic of the oscillatory motion U_{osc} far from the bottom, equals $1/\hat{U}_1^*$, according to (19) which in turn can be written as $1/\hat{u}_{d1}^*(z_o^*)$. According to a similar reason, the phase lag Ψ_1 between p_{b1} and U_1 equals minus the phase lag between p_{b1}^* and $u_{d1}^*(z_o^*)$. Thus, from the computer results with the mentioned bottom boundary conditions, the choice of a value of z_o^* gives a relationship between a value a_1/r and the belonging values of $\hat{p}_{b1}/\hat{U}_1$ and Ψ_1. By using z_o^* as a parameter, the general relationship between a_1/r and the last mentioned parameters can be obtained; this is shown in Fig. 1. The same results are plotted in another way in Fig. 2, giving $\hat{U}_1^*$ (= $\hat{u}_{d1}^*$ at z_o^*) and Ψ_1 as a function of z^*.

Now the attention will be turned to the mean velocity profile $\bar{u}$ as function of z. From (10) and (18) for the upper part of the mean velocity profile is found:

$$\bar{u} = \bar{U} + \frac{\sqrt{\bar{\tau}/\rho}}{K} \ln \frac{z}{z_{max}} \quad \text{for } z \geq z_{max} \tag{26}$$

where $\bar{U}$ is the mean velocity at $z = z_{max}$. Averaging (16) over the wave period and integrating, one finds in the vicinity of the bottom, where $\bar{p} \approx \bar{p}_b$:

$$\bar{u} \approx \frac{\bar{p}_b}{K} \ln \frac{z}{z_o} \quad \text{(near the bottom)} \tag{27}$$

Therefore, plotting $\bar{u}$ on the horizontal scale versus $\ln z$ on the vertical scale, the upper part will be a straight line with a gradient arctan $(K/\sqrt{\bar{\tau}/\rho})$, where the curve tends to a straight line with gradient arctan $(K/\bar{p}_b)$ near the bottom. The last-mentioned gradient is larger than the first-mentioned one: the ratio $\bar{p}_b/\sqrt{\bar{\tau}/\rho}$ will be called β_{ob} and equals approximately $\sqrt{\pi \bar{p}_b^*/4}$ (for $\bar{p}_b^* << 1$); this follows from substitution of[2] $p_b = \bar{p}_b + \hat{p}_{b1} \sin\omega t$ into (15) and approximating in an analytical way[2,3].

---

[1] This has been done earlier by Bakker (1974). In the present paper the conception is left of a coefficient "f_w", occurring in the former paper, which relates the top-bottom shear stress to the top-orbital velocity. Because of the effect of higher harmonics, this coefficient obscures rather than enlightens the mechanism.

[2] This result has already been used for the transition from (22) to (23).

[3] Bakker (1979); Bakker and Van Doorn (1979).

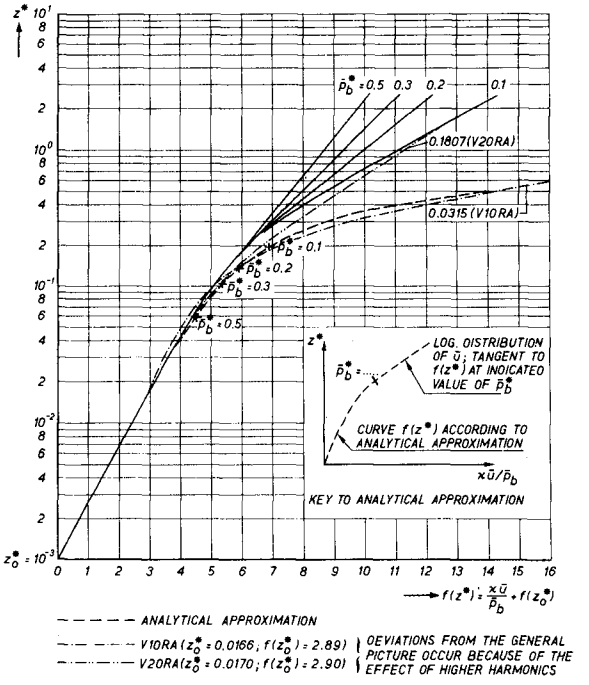

Fig.3a. Theoretical distribution of mean velocities.

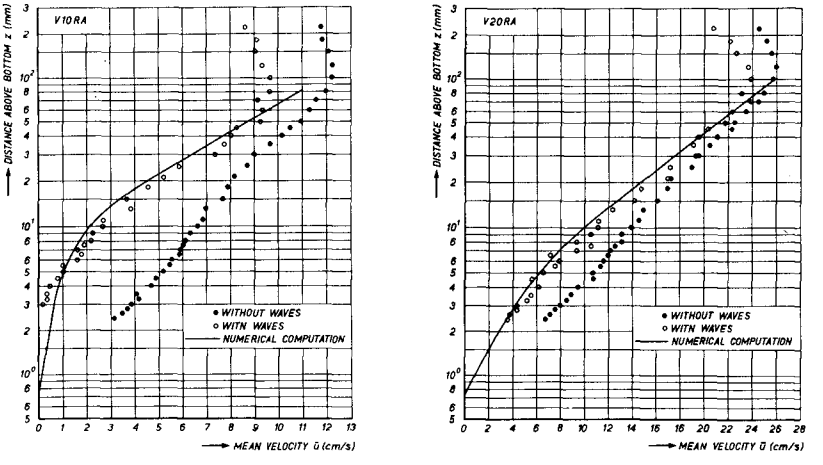

Fig.3b. Comparison with measurements.

Fig.3. The mean velocity distribution according to theory and measurements.

Thus it shows, that the velocity profile consists of two logarithmic parts with a transition zone between.

With respect to this transition between the bottom and $z = z_{max}$, an analytical approximation[1] suggests the occurrence of a universal function $f(z^*)$ in this way, that for small values of z^* the following relationship holds:

$$\frac{\kappa \bar{u}}{\bar{p}_b} = f(z^*) - f(z_o^*) \tag{28}$$

When z^* is plotted on a vertical, logarithmic scale and $\kappa\bar{u}/\bar{p}_b$ on a linear horizontal scale so that 1 on the horizontal scale corresponds with $\ln e$ on the vertical scale, the lower part of the curve $f(z^*)$ degenerates to a line under an angle of 45°. Thus this part corresponds with the lower logarithmic part of the velocity profile mentioned before. The curve $f(z^*)$ also gives the transition zone; the upper logarithmic part of the velocity profile can be found by drawing the tangent to $f(z^*)$ with a gradient $\sqrt{\pi \bar{p}_b^* /4}$ with the horizontal (inset Fig. 3).

From the computer results the curve $f(z^*)$ can be found. Starting from certain values of $\bar{p}_b^*$ and assuming $\hat{p}_{b2}^*$ and $\hat{p}_{b3}^*$ equal to zero, the velocity field u_d^*, and thus $\bar{u}_d^*$, can be calculated; starting from a certain, rather arbitrary[2] value of z_o^*, one can find $\bar{u}^*$, and thus $\kappa\bar{u}^*/\bar{p}_b^*$, equal to $\kappa\bar{u}/\bar{p}_b$. Indeed it shows, that the lower part of the resultant curves for various values of $\bar{p}_b^*$ coincide, and that the lower part gives a straight line under 45°, whereas the upper parts show a gradient $\sqrt{\pi \bar{p}_b^* /4}$ (Fig. 3a).

The question remains how $\bar{p}_b$ can be determined from U_{mean}, the velocity averaged over the period as well over the depth h.

Without an oscillatory motion, the relationship would exist:

$$\bar{p}_b = \frac{\kappa U_{mean}}{\ln (h/ez_o)} \quad \text{(without oscillatory motion)} \tag{29}$$

which can be derived in the same manner as the Chezy relationship[3].

With oscillatory motion, an approximate calculation of U_{mean} from $\bar{p}_b$ (or inversely: of $\bar{p}_b$ from U_{mean}) could be made by neglecting the effect of the transition zone and the lower logarithmic curve on the mean velocity and extrapolating the upper logarithmic curve in downward direction (Fig. 4). However, this extrapolated line will intersect the (vertical) line of zero-velocity, in a point higher than $z = z_o$, say $z = \alpha z_o$ (Fig. 4). Thus it shows, that the effect of the oscillatory motion is an enlargement of the apparent roughness with a factor α. Furthermore, $\bar{p}_b$ in (29) should be replaced by $\sqrt{\bar{\tau}/\rho}$, which makes a difference of a factor β_{ob}, as stated before in this Chapter. Thus, in case of oscillatory flow, (29) changes into:

$$\bar{p}_b = \frac{\beta_{ob} \kappa U_{mean}}{\ln (h/e \alpha z_o)} \tag{30}$$

---

1) Bakker (1979); Bakker and Van Doorn (1979)

2) Only should be conditioned, that z_o^* is so small, that it gives a point on the lower straight section (under 45°) of the $f(z^*)$-curve.

3) This can be easily seen by multiplying both sides of Eq. (29) with $(1/\kappa)\ \ln (h/ez_o)$.

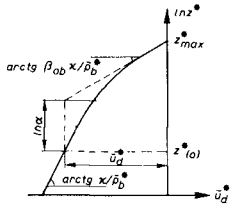

Fig.4. Relationship between $\ln \alpha$ and $\bar{u}_d^*$

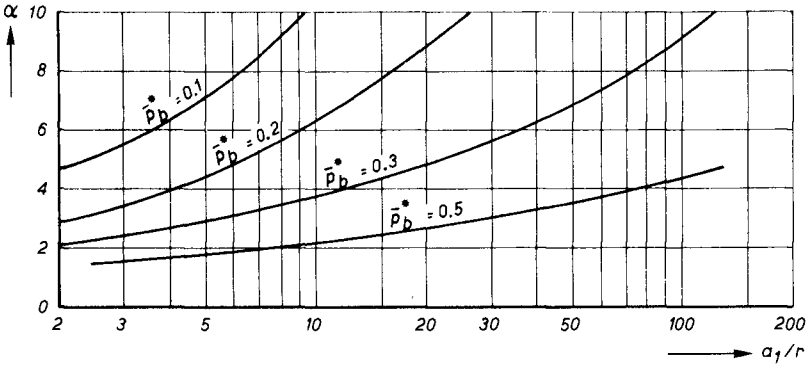

Fig.5. The coefficient α as function of a_1/r and $\bar{p}_b^*$.

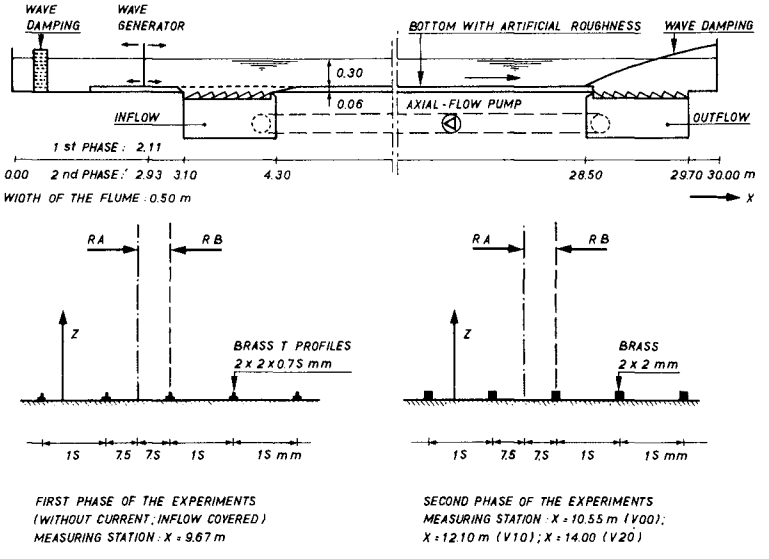

Fig.6. Wave flume and artificial roughness.

in which $\beta_{ob} \approx \sqrt{\pi \bar{p}_b^* / 4}$ [1] and in which α is derived with the aid of the computer program in the following way.

Analogous to the case with the first harmonic, each level z^* can be considered as a lower boundary condition z_o^*, which determines a_1/r. Fig. 4 shows that α can be found from the following relationship:

$$\ell n\, \alpha = \ell n \frac{z^*_{max}}{z^*} - \frac{\beta_{ob}\kappa}{\bar{p}_b^*} \cdot \bar{u}_d^*(z^*) \qquad (31)$$

where $\bar{u}_d^*(z^*)$ denotes $\bar{u}_d^*$ at the level z^*. In this way, with one computer calculation -starting from a bottom boundary condition with a certain value of $\bar{p}_b^*$ and assuming $\hat{p}_{b2}^*$ and $\hat{p}_{b3}^*$ equal to zero- one may find the value of α for a great number of values a_1/r. Fig. 5 shows α as a function of a_1/r and $\bar{p}_b^*$.

Now the following rough way of calculation of the mean velocity profile is advised:

a. Determine a_1/r, using $a_1 = \hat{U}_1 T/2\pi$
b. Determine $\hat{p}_{b1}$ from the ratio $\hat{p}_{b1}/U_1$, found in Fig. 1
c. Calculate $\bar{p}_b^*$ from (30), which may be written as:

$$\bar{p}_b \approx \frac{\pi}{4} \cdot \left[\frac{U_{mean}}{(\hat{p}_{b1}/\kappa)\ \ell n\ (h/e\alpha z_o)}\right]^2 \quad \text{(see note 2)} \qquad (32)$$

Here α has to be determined iteratively: assuming for instance first $\alpha = 1$, finding $\bar{p}_b^*$ from (32), finding a better estimation of α from Fig. 5 until the wanted accuracy of $\bar{p}_b^*$ is reached.

d. The lower part of the profile is a straight line on single-logarithmic paper under an angle arctan $(\kappa/\bar{p}_b)$ through the point $(u,z) = (o,z_o)$
   . the upper part is a straight line on single-logarithmic paper under an angle arctan $(\beta_{ob}\ \kappa/\bar{p}_b)$ or, approximately arctan $(\kappa\sqrt{\pi/(4\bar{p}_b\ \hat{p}_{b1})})$
   . the transition can be found from Fig. 3a.

As mentioned, more accurate results can be obtained by using the computer program directly; in this case a first estimation of $\bar{p}_b^*$ follows from (32).

4 Numerical accuracy

A number of computations has been carried out in order to check the numerical accuracy. For the details is referred to Bakker and Van Doorn (1979); here the following results may be mentioned.

a. In the computer program an initial condition can be introduced, which may be different from the one, following from the periodical bottom boundary condition. After 4 periods running, the effect of this initial condition vanished up to 1°/oo of $\hat{p}_{b1}$ [3].
b. The effect of the upper boundary condition on the ratio $\hat{p}_{b1}/\hat{U}_1$ is small, as long as z^*_{max} is 1.5 at least.

---

[1] For $\bar{p}_b^* > .5$ this approximation becomes inaccurate, in which case is referred to Bakker (1979) or Bakker and Van Doorn (1979).

[2] In (32) the denominator between the brackets shows a hypothetical mean velocity over the profile, which would occur when the bottom shear stress velocity would have been $\hat{p}_{b1}$, instead of (a mean value of) $\sqrt{\bar{\tau}/\rho}$. and when the roughness would have been αr instead of r.

[3] The ratio between $\hat{p}_{b1}$ and $\hat{U}_1$ can be found from Fig. 1.

c. The greatest traceable source of numerical error in the program is found to be caused by the fact, that the present iteration procedure does not extend up to the fourth and fifth harmonic; when the real fourth and fifth harmonic of U are zero, the error is of the order of 20% of $\hat{p}_{b1}$. Because of this error, the accuracy is not effectively enlarged by taking more than 6 grids (using $z^*_{max} = 1.5$). The differences in U_1 between the use of respectively 3, 4, 5 grids compared with using 6 grids is respectively 4, 2, 1, 0.3% of $\hat{U}_1$ when $a_1/r = 129$ [1]). The raising of the grid number by 1 increases the computer time about a factor 2.

d. Considering the case without resultant current, the effect of a third harmonic of p_b (being so large, that $\hat{U}_3$ becomes zero) on the first harmonic U_1 is small (about 1% of $\hat{U}_1$).

e. The effect of $\bar{p}_b$ (i.e. resultant current) on the first harmonic u_{d1} is relatively small for large values of a_1/r (2.5% of $\hat{U}_1$ when $a_1/r = 129$ and $\bar{p}^*_b = .23$). For smaller values of a_1/r the effect is larger (6% of $\hat{U}_1$ when $a_1/r = 3.5$ and $\bar{p}^*_b = .23$).

5 Experiments

The bottom boundary layer under periodic progressive water waves, without and with a superimposed current has been investigated at the Delft Hydraulics Laboratory (DHL). The results of these experiments on the velocity distribution are compared with the present theory. In the theory, assumptions are made for the case of a horizontally oscillating flow such as can be realized in a horizontally pulsating water tunnel. The results of the present investigations, with free surface waves, will in future be compared with results from similar tests in the Oscillating Water Tunnel of the DHL.

Water surface elevation (η) and horizontal water velocity component in the direction of wave propagation (u) have been measured simultaneously in the same cross-section in a 30 m long, 0.5 m wide and 0.5 m high glass-walled flume of the DHL (Fig. 6).

Periodic waves were generated by a flat wave board oscillating horizontally with adjustable amplitudes at the lower and upper side. The wave trains applied in the experiments, obtained by starting the wave generator always from the same position were very well reproducible. In all experiments, the still-water depth (h) was 0.30 m, the wave period (T) with respect to a fixed point 2.0 s and the wave height (H) at the measuring station 0.12 m. Steady currents can be generated by circulating the water (Fig. 6). In view of the presence of secondary waves, the measuring stations were chosen so that the ratio of the amplitudes of the first and second harmonic components of the surface waves approximately showed a maximum. In order to obtain a turbulent boundary layer at the bottom, two-dimensional roughness elements (2 mm high at 15 mm centers) were applied (Fig. 6).

---

[1]) In the present program z^*_o may differ from Δz^*. This is a facility, plugged in the computer program after Appendix A of Bakker (1974) was written. In this way the value of $\hat{U}^*_1$ belonging to an arbitrary value of a_1/r can be calculated, independent of the number of grids. For details, cf. Bakker and Van Doorn (1979).

The experimental study has been performed in two phases. In the first phase [1], waves without a current were considered. The inflow provision in the flume was covered. The artificial bottom roughness was applied only over a distance of 1.5 m at the measuring section.
In the second phase of the experiments [2], roughness elements were applied over a distance of 15 m next to the water inlet and currents were generated in the same direction as the wave propagation. The mean current velocities (averaged over the height) were approximately 0.10 m/s (test code V10) and 0.20 m/s (test code V20). In this second phase, tests without a current (test code V00), but with open inlet were repeated for comparison.

For each condition, velocities in two verticals have been measured viz. in between two roughness elements (code RA) and just above one (code RB). In this way, tests series were performed with codes RA, RB (first phase) and V00RA, V00RB, V10RA, V10RB, V20RA, V20RB (second phase).

Figure 3b shows the distribution along the vertical of measured current velocities (time average values). It is noted that in the experiments the speed of the pump was the same for the current only and for current with waves, whereas the theory on oscillatory flow with resultant current starts from a given gradient of the mean water level which is supposed to be the same for "current only" and for "current with waves".

For the analysis, only the waves from a wave train were used after the start-up transients and before the first reflected wave reached the measuring station. Three wave trains were applied for every level at which velocities have been measured, from which as an average a more accurate orbital velocity could be determined. In the case of waves with a current, η and u are measured also without waves.

The water surface elevation was measured with a resistance-type wave gauge. The velocities were measured at a series of successive levels above the bottom with a laser-doppler velocity meter (LDV). The application of this technique with its general advantage of measuring accurately and contactless in very small measuring volumes, was highly satisfactory. The error in positioning the level of the LDV was less than +/- 0.1 mm. The reference distance to the bottom, determined by means of a measuring rule is less accurate; the error is estimated less than +/- 0.3 mm.

The signals from the wave gauge and the LDV were recorded simultaneously on paper and on an analog magnetic tape. From the tape recorder the signals have been processed in two steps:

a. Digitization by synchronized sampling, exactly 72 times per wave period, i.e. a sampling frequency of 36 Hz. From every wave train, the measured signals have been sampled over the same time interval after the start of the wave generator, so phase relations between velocities measured at different levels could be maintained. In the first phase of the experiments, the accuracy of digitizing was +/- 0.025 cm and +/- 0.15 cm/s for the signals of the surface waves and the velocities respectively. In the second phase, these values were 10 times smaller.
b. Harmonic analysis of the digital signals. The results obtained from harmonic analysis of the average wave (i.e. also velocities) of the three wave trains were used for comparison with theory.
Table 1 shows the most important parameters deduced from the tests.

---

[1] Van Doorn and Godefroy (1978)

[2] Van Doorn (1979)

TEST	$\hat{U}_1$ (1) (cm/s)	$\bar{U}$ (2) (cm/s)	s_1 (3) (mm)	a_1/r (4)	Z (5) (mm)	$\hat{p}_{b1}$ (6) (cm/s)	$\bar{p}_b^*$ (7)	β_{ob} (8)	$\hat{p}_{b2}$ (9) (cm/s)	$\hat{p}_{b3}$ (10) (cm/s)	ψ_1 (11) (degr.)	ψ_2 (12) (degr.)	ψ_3 (13) (degr.)
RA RB	29.83	-2.6	95.0	4.11	49.8	6.22	-0.054		1.33	1.03	49.5	191.1	0.2
V0ORA V0ORB	26.5	-3.0	84.5	3.65	45.8	5.72							
V1ORA V1ORB	25.7	9.6	81.8	3.54	44.7	5.58	0.0315	0.095	1.46	1.18	53.1	196.7	343.7
V2ORA V2ORB	24.3	22.7	77.3	3.35	41.5	5.19	0.1807	0.329	1.35	1.23	52.7	193.1	331.3
JONSSON ('63) (cf. Ch. 6)	211	0.5	2850	112.8	697.8	20.79	0.0121		0.96	1.49	25.4	305.6	76.3

(1) $\hat{U}_1$ = amplitude of the 1st harmonic of the velocity just outside the boundary layer
(2) $\bar{U}$ = mean velocity at $z = z_{max} = 1.5\ Z$
(3) $a_1 = \hat{U}_1 T/2\pi$; (4) $r = 33\ z_o$; (5) $Z = \kappa\ \hat{p}_{b1} T$
(6)-(13) These values have been adopted from the numerical solution
(8) $\beta_{ob} = \bar{p}_b/\sqrt{\bar{\tau}\rho}$

Table 1 Test parameters

6 Comparison between theory and measurements

Comparison is made between the theory and the measured mean velocity profiles V1ORA and V2ORA. The results are plotted in Fig. 3b.

The theoretical curves (found from the computer program) differ from the ones which can be interpolated, using Fig. 3a, because of the effect of the strong second harmonic U_2 (about 1/3 of the first harmonic U_1) on $\bar{\tau}$, which is not taken into account in the derivation of Fig. 3a.

With respect to the comparison of the first harmonic, apart from the experiments, mentioned in Ch. 5, also the measurements of Jonsson (1963) (see also Jonsson and Carlsen, 1976) will be taken into consideration for the comparison between theory and measurements. The experimental data, as derived from the literature are added to Table 1.

For the various experiments, the dimensionless amplitude and the phase of the defect velocity have been calculated and plotted against the dimensionless height above the bottom. The results are shown in Fig. 2. With respect to the amplitude of the defect velocity there is a rather good agreement between measurements and theory, whereas the phases still show discrepances.

The comparison between the instantaneous velocity profiles according to the theory and the measurements (starting from a given upper boundary condition) is given in Figure 7.

The general trend is rather well predicted, although the "overshoot" velocity tends to be higher according to the measurements than according to theory. Fig. 8 shows $\sigma(u)/\hat{p}_{b1}$ as function of the dimensionless distance z^* above the bottom for the various tests, $\sigma(u)$ being the standard deviation between the theoretical and measured values of the instantaneous velocities at a certain height. The mean value $\bar{\sigma}$ of $\sigma(u)$, averaged

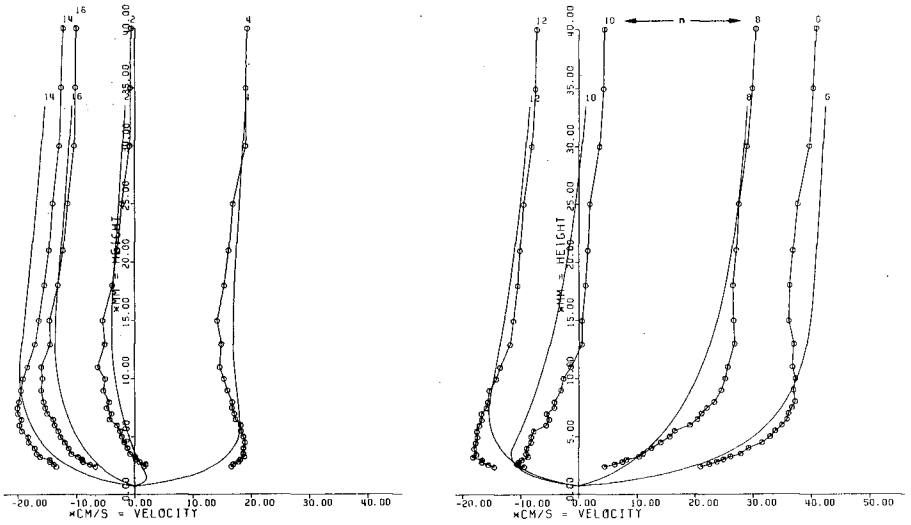

Fig.7a. V10RA $\bar{\sigma}$= 2.39 cm/s

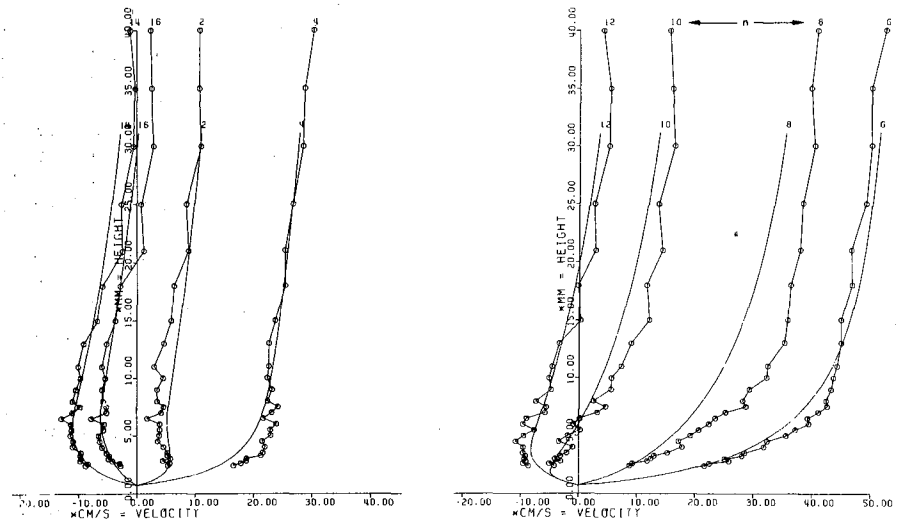

Fig.7b. V20RA $\bar{\sigma}$= 2.27 cm/s

Fig.7. Instantaneous velocity profiles according to theory and measurements.

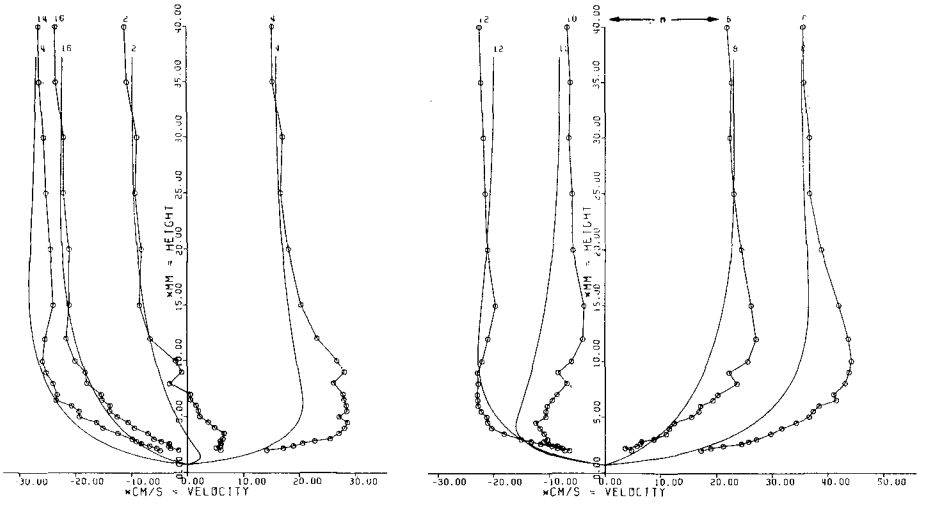

Fig.7c. RA $\bar{\sigma}$= 4.71 cm/s

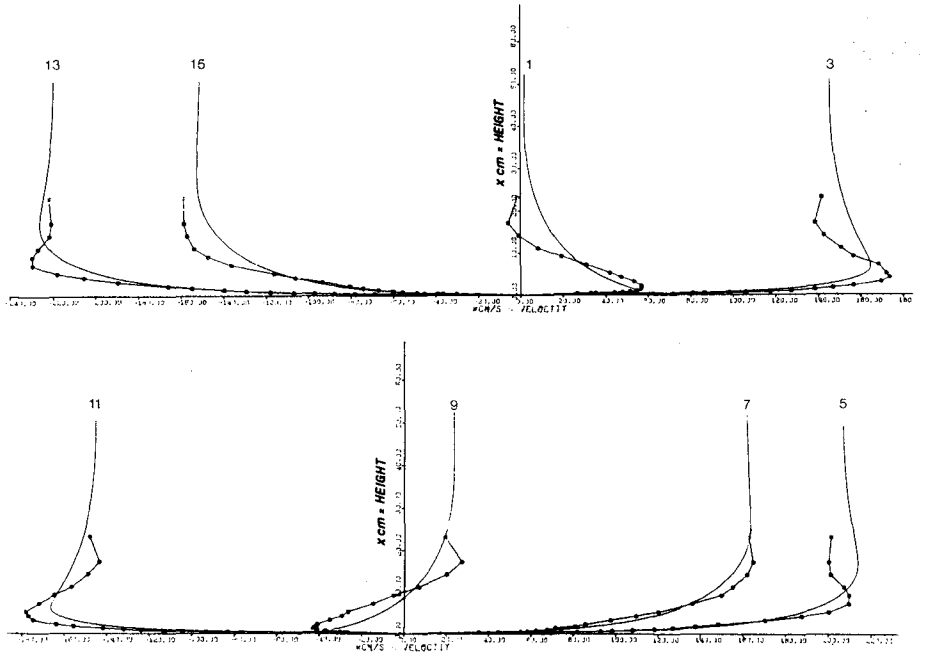

Fig.7d. JONSSON (1963) $\bar{\sigma}$= 10.79 cm/s

Fig.7. Instantaneous velocity profiles according to theory and measurements.

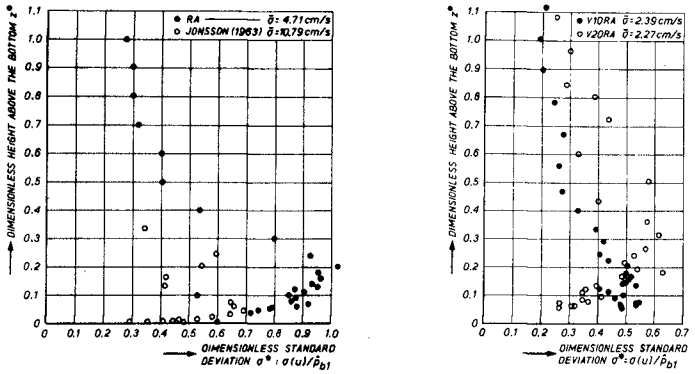

Fig.8. Dimensionless standard deviation as function of the dimensionless distance above the bottom.

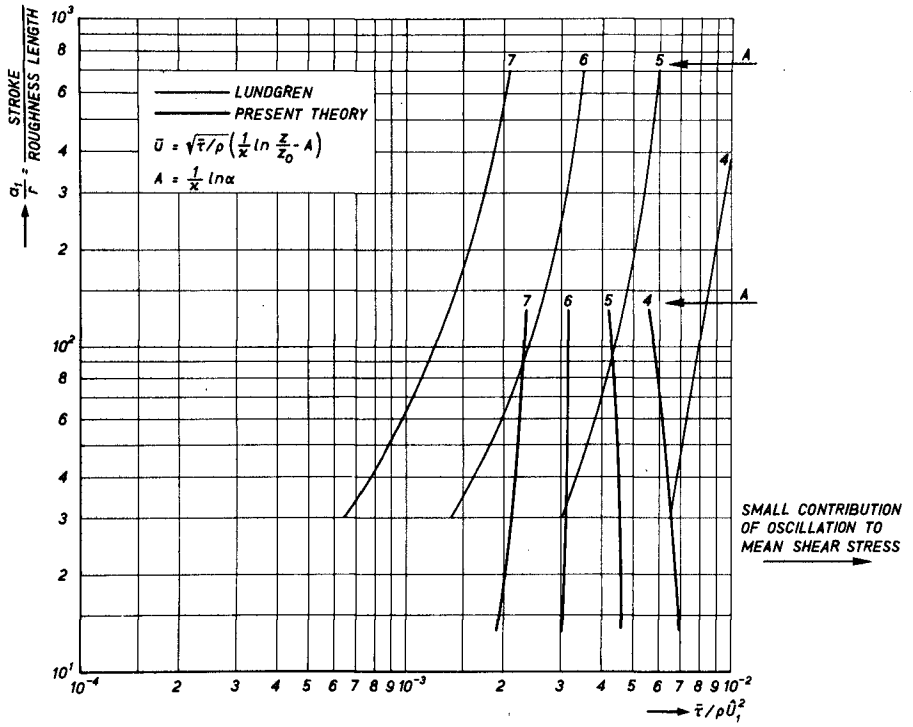

Fig.9. Comparison of the velocity defect according to Lundgren and the present theory.

over the considered levels within the boundary layer, has also been given in Figs. 7 and 8.

7 The mean velocity profile according to the present theory and according to Lundgren

Lundgren (1972) defines a shear stress velocity "U_f" (Eq. (19) of his paper), equal to τ_{cw}/ρ, in which "τ_{cw}" is the period-average of the bottom shear caused by waves and current. Thus "U_f" equals $\bar{p}_b/\beta_{ob}$ in the present notation.

Lundgren's equation ((23) of his paper) for the mean velocity profile reads, in the notation of the present paper:

$$\bar{u} = \frac{\bar{p}_b}{\beta_{ob}}\left(\frac{1}{\kappa}\,\ell n\,\frac{z}{z_o} - A\right) \tag{33}$$

in which he calls A the "velocity defect".

In the present theory, the upper part of the velocity profile is given by:

$$\bar{u} = \frac{\bar{p}_b}{\beta_{ob}\kappa}\,\ell n\,\frac{z}{\alpha z_o} \qquad (z >> z_o) \tag{34}$$

Therefore "A" equals $(\ell n\alpha)/\kappa$. In his Fig. 2 Lundgren presents as result of his calculations the value of A as function of "$\tau_{cw}/\rho U_b^2$", being in the present notation $\bar{\tau}/\rho\hat{U}_1^2$, or in dimensionless notation $(\bar{p}_b^*/\beta_{ob}\hat{U}_1^*)^2$.

In the computer program, $\bar{p}_b^*/\beta_{ob}$ is known from the upper boundary condition (22). In the computer program for given values of $\bar{p}_b^*$ as well A as $\bar{\tau}/(\rho\hat{U}_1^2)$ can be calculated as function of a_1/r; therefore Fig. 2 according to the lay-out of Lundgren may be reproduced according to the present theory. In Fig. 9 the lines of constant "A" as function of a_1/r and $\bar{\tau}/\rho\hat{U}_1^2$ according to Lundgren and the present theory are drawn together.

8 Summary and conclusions

a. Bakker (1974) presented a numerical mathematical model of the turbulent bottom boundary layer in periodic waves with (or without) resultant current in the direction of wave propagation. This model starts from the Prandtl assumptions with respect to the relationship between shear stress and the instantaneous velocity gradient. Non-linear interactions are taken into account.

b. In the present paper the mathematical model has been improved and has been compared with experimental investigations at the Delft Hydraulics Laboratory (DHL). Velocities at a series of successive levels above the bottom under free surface waves without, respectively with resultant current in a wave flume were measured with a laser-doppler velocity meter.

c. The mathematical model predicts reality rather well although the phases of the first harmonic of the "defect velocity" in model and reality show discrepances. With respect to the resultant velocity is referred to Fig. 3, with respect to the amplitude and phase of the first harmonic of the defect velocity to Fig. 2 and with respect to the instantaneous velocity profiles to Fig. 7. In Fig. 8 the standard deviation between measurements and theory is given as a function of the height above the bottom in a dimensionless graph. For this, $\hat{p}_{b1}$ has been used as reference velocity (the ratio between $\hat{p}_{b1}$ and the amplitude $\hat{U}_1$ of the first har-

monic of the velocity outside the boundary layer is given in Fig. 1) and $\kappa\hat{p}_{b1}T$ as a reference height.

d. The shear stress, exerted at the bottom according to this model and according to the investigation of Lundgren (1972) appears to be of the same order of magnitude (Fig. 9), although the problem is approached from a different angle.

e. In the future, the mathematical model will be improved by including higher harmonics than the third in the upper boundary conditions; the measurements will be continued with similar tests in the Oscillating Water Tunnel of the DHL; a (less accurate) analytical theory will be presented, giving more insight in the physics of the matter.

9 Acknowledgement

The authors gratefully acknowledge the important remark of Mr. J. van Overeem, mentioned before. Furthermore, the contribution of Mr. C.J. van Kakum in programming and the valuable assistance of Mr. J. van Overeem and Mr. W. Tilmans should be mentioned. The authors thank Mr. C. Fischer for his linguistic remarks.

References

- BAKKER, W.T. (1974).
Sand concentration in an oscillatory flow.
Proc. 14th Conf. on Coastal Engineering, Copenhagen.
- BAKKER, W.T. (1979).
Analytical computations on the near-bottom velocity field in waves with a current (in preparation).
- BAKKER, W.T. and DOORN, Th. van (1979).
Bottom friction and velocity distribution in an oscillatory flow with resultant current (in preparation).
- DOORN, Th. van and GODEFROY, H.W.H.E. (1978).
Experimental investigation of the bottom boundary layer under periodic progressive water waves.
Report M 1362 (2 parts) of the Delft Hydraulics Laboratory.
- DOORN, Th. van (1979).
Experimental investigation of near-bottom velocities in water waves without and with a current.
Report M 1423 of the Delft Hydraulics Laboratory (in preparation).
- JONSSON, I.G. (1963).
Measurements in the turbulent wave boundary layer.
Proc. of the 10th IAHR Congress, London.
- JONSSON, I.G. and CARLSEN, N.A. (1976).
Experimental and theoretical investigations in an oscillatory turbulent boundary layer.
Journal of Hydraulic Research, Vol. 14, No. 1, pp. 45-60.
- LUNDGREN, H. (1972).
Turbulent currents in the presence of waves.
Proc. 13th Conf. on Coastal Engineering, Vancouver.
- PRANDTL, L. (1931).
Abrisz der Strömungslehre, Braunschweig, 3er Abschnitt.

LIST OF SYMBOLS

a_1	stroke length $\hat{U}_1 T/2\pi$
e	basic number of neperian logarithms
$f(z^*)$	universal function, from which $\kappa\bar{u}/\bar{p}_b$ can be found (vide (28))
h	water depth
ℓ	mixing length (schematized according to (7))
ℓ_{real}	more realistic value of mixing length
p	internal shear stress velocity ($\sqrt{\tau/\rho}$) in the fluid
p_r	(instantaneous value of the) water pressure
r	Nikuradse roughness
t	time
T	wave period
u	horizontally directed water velocity (uniform in horizontal direction), after averaging turbulent fluctuations
U	velocity u at $z = z_{max}$
u_d	"defect velocity" $u - U$
U_{mean}	mean velocity, averaged over both wave period T and water depth h
U_{osc}	oscillatory water motion above the boundary layer (assumed uniform over the height), i.e. $u - \bar{u}$ for $z \geq z_{max}$
x	horizontal coordinate
z	vertical coordinate
z_o	r/33, the theoretical level where the velocity is assumed to be zero
z_{max}	height, at which the variations of the internal shear stress are attenuated
α	multiplication factor of the apparent roughness, caused by the addition of the oscillation to the current
β_o	ratio between $\bar{p}$ and $\sqrt{\bar{\tau}/\rho}$ (about equal to $\sqrt{\pi \bar{p}_b^*/4}$ if $\bar{p}_b^* \ll 1$ and if $\hat{U}_{2,\ldots} \ll \hat{U}_1$)
κ	Von Karman constant
ρ	specific density
τ	internal shear stress in the fluid
$\bar{\tau}_{real}$	more realistic approximation of the shear stress averaged over the wave period than $\bar{\tau}$ (vide (4))
$\phi_{2,(3)}$	phase angle of harmonics of the shear stress velocity p
$\Psi_{1,(2),(3)}$	phase angle of harmonics of the velocity U at height $z = z_{max}$ above the boundary layer
ω	angular frequency of first harmonic of oscillation ($2\pi/T$)

Other symbols added to a variable x:

$\bar{x}$	average value of x during period T
x^*	"dimensionless variable", i.e. velocity divided by $\hat{p}_{b1}$, or height divided by $\kappa\hat{p}_{b1}T$, or time, divided by T
x_b	value of x at the bottom (z = 0)
$x_{1,(2),(3)}$	subscript applies to first, (second), (third) harmonic of x
$\hat{x}$	amplitude of harmonic x (always in combination with subscript 1, 2 or 3)
$\|x\|$	absolute value of x
sign(x)	"+1" if x is positive, "-1" if x is negative
X(x)	value of variable X at height x